Optical benchmarking of security document readers for automated border control

Kristián Valentín, Peter Wild, Svorad Štolc, Franz Daubner and Markus Clabian

Digital Safety & Security Department, AIT Austrian Institute of Technology GmbH, Donau-City-Str. 1, 1220 Vienna, Austria

ABSTRACT

Authentication and optical verification of travel documents upon crossing borders is of utmost importance for national security. Understanding the workflow and different approaches to ICAO 9303 travel document scanning in passport readers, as well as highlighting normalization issues and designing new methods to achieve better harmonization across inspection devices are key steps for the development of more effective and efficient next-generation passport inspection. This paper presents a survey of state-of-the-art document inspection systems, showcasing results of a document reader challenge investigating 9 devices with regards to optical characteristics.

Keywords: Security documents, MRTD inspection, document readers, automated border control

1. INTRODUCTION

EU border agency Frontex initiated document challenges in 2012 and 2013 analysing passport inspection performance of human experts and machines in first-line border control. Experiments highlighted a high degree of variability and inconsistency leading to system errors (false accepts/rejects) in automated solutions.[1] Both overreliance and unfounded mistrust of border guards when using inspection devices were identified. Therefore, Frontex recently clearly emphasized the need for standardised approaches built on reference knowledge recommending the development of unified testing methodology and vendor-independent reference document and template databases.[2] This paper strives at providing a useful tool for document inspection system manufacturers in their efforts to facilitate modular solutions and harmonized usage. In this context it is important to differentiate between automated border crossing using self-service eGates and manual inspection supporting border guards in their assessment. Limitations with regards to automated inspection are identified and recommendations for enhanced interoperability are given.

The contribution of this work to the state-of-the-art in document inspection is threefold: First, the paper provides a survey of existing technologies in digital passport scanning and optical inspection. Requirements and potential future means of automated document verification are analysed. Second, the paper reports on a document reader challenge testing interoperability of hardware (see Fig. 1) with regards to image quality and optical characteristics, elaborating on advantages and disadvantages of applied technologies. Third, the paper concludes with recommended requirements (calibration, hardware, etc.) for automated border crossing.

The paper is organised as follows: Section 2 introduces state-of-the-art solutions of document scanning, followed by an overview of document inspection technologies. Results of the conducted document challenge are reported in Section 3. Finally, Section 4 gives an outlook and forms the conclusion.

2. OPTICAL DOCUMENT READERS

With the introduction of machine-readable e-passports by ICAO with the 9303 standard[3] in 1980 and means to digitally read a travel document's machine-readable zone (MRZ) and chip data integrated within the document (access to holder's personal data, including biometrics), several manufacturers have started to develop document inspection devices assisting border guards in verifying authenticity. There are many research reports on electronic authentication and related radio-frequency identification (RFID). Among the first, Ness[4] described a system for

Further author information:
E-mail: {kristian.valentin, peter.wild, svorad.stolc, franz.daubner, markus.clabian}@ait.ac.at

3M AT9000 MK2 | ARH Combo Smart | ARH PRMc | Bundesdruckerei VE 600 | DESKO ICON Gen I

DESKO PENTA Gen 4.0 | Regula 7024m.111 | Regula 7034.111 | Suprema RealPass-V

Figure 1: Overview of document inspection systems under test.

Table 1: Supported features as claimed by vendors of tested readers (✓ yes, – no, ○ optional, ? unknown).

	Camera					Light		RFID				OCR			Integrity					Security Verification									Images			
	Resolution (DPI)	Width (mm)	Height (mm)	Anti-Gloss	Photo-Cam	Vis-W, IR, UV-A	Visible-Red	ICAO 9303	BSI TR-03105 4	BSI TR-03105 5.1	BSI TR-03105 5.2	ICAO MRZ	ID 1/2/3 doctype	VIZ	MRZ checksum	MRZ vs. VIZ	Expiry	RFID vs. VIZ	RFID vs. face	UV dull	UV fibers	Retroreflectivity	Microprinting	IPI	Holograms	OCR-B font	B900 ink	IR transp.	Visible, IR, UV	Reflections (OVD)	Glare-free Vis/IR	Face (highres)
3M AT9000 MK2	400	125	88	✓	–	✓	–	✓	?	✓	–	✓	✓	–	✓	○	○	✓	○	✓	–	○	–	–	–	–	✓	–	✓	–	✓	–
ARH Combo Smart	500	125	88	✓	–	✓	–	✓	–	–	–	✓	✓	✓	✓	–	✓	✓	✓	✓	–	–	–	–	–	–	✓	–	✓	✓	✓	–
ARH PRMc	500	130	98	✓	✓	✓	–	✓	–	–	–	✓	✓	✓	✓	–	✓	✓	✓	✓	–	–	✓	✓	–	–	✓	–	✓	✓	✓	✓
Bundes-druckerei VE 600	400	128	96	✓	–	✓	✓	✓	✓	✓	✓	✓	✓	✓	✓	○	✓	○	○	✓	○	–	–	○	–	✓	✓	✓	✓	–	✓	–
DESKO ICON Gen I	500	131	94	–	–	✓	–	✓	✓	✓	✓	✓	✓	○	–	–	–	–	–	–	–	–	–	–	–	–	–	–	✓	–	–	–
DESKO PENTA Gen 4.0	500	131	94	–	–	✓	–	✓	✓	✓	✓	✓	✓	○	–	–	–	–	–	–	–	–	–	–	–	–	–	–	✓	–	–	–
Regula 7024m.111	380	128	88	✓	–	✓	–	✓	–	✓	✓	✓	✓	✓	✓	✓	✓	✓	✓	✓	✓	✓	✓	✓	✓	✓	✓	✓	✓	✓	✓	–
Regula 7034.111	400	128	88	✓	–	✓	–	✓	–	✓	✓	✓	✓	✓	✓	✓	✓	✓	✓	✓	✓	✓	✓	✓	✓	✓	✓	✓	✓	✓	✓	–
Suprema RealPass-V	420	130	90	–	–	✓	–	✓	?	?	?	✓	✓	✓	✓	–	✓	✓	–	✓	✓	–	–	–	–	–	✓	–	✓	–	–	–

electronic passport verification. Recently, Butt et al.[5] investigated duplicate enrollment checks suggesting protocols to prevent illegitimate issuance of passports and Hamad et al.[6] presented an RFID-based Location Authentication Protocol for passport detection and verification. While e-Passport technology heavily relies on RFID-based authentication (Monnerat et al.[7] provide a good survey), and biometrics for authentication,[8] optical document inspection has not yet received a lot of attention despite the fact devices also support border guards in their validation of a passport's security features.

Assuming printed security patterns can not easily be reproduced, a series of vendors have suggested automated systems for document authentication, see also Table 1 for a list of devices with corresponding claimed features (including an unsorted list of security features). Dolev[9] developed a system authenticating a document by processing visible data zone (VIZ) sections using a template-driven engine, and Blair[10] patented a method for document authentication using illumination from multiple spectra. Modern document readers all acquire multispectral images for inspection of security-features in different bands: near-infrared NIR, visible colour VIS and ultra-violet-illuminated UV(-A) at resolutions of approximately 350 to 500 dots per inch (DPI). Additional inspection of security features is important, as several known attacks on electronic verification constitute a threat to security, for example: forging, skimming, and eavesdropping.[11]

Security features can be attributed to paper (e.g., fluorescent fibres), substrate (e.g., dull material), background and text print (e.g., unique fonts), ink (e.g., infrared visible/dropout ink) copy protection (e.g., optically variable devices) and counter-alteration (e.g., steganographic features). The selection of type, position and appearance of security features is defined by the issuing authority. Special attention in document image acquisition should be given to glare (including gloss/specular reflections) sensed in visible spectrum as mostly undesirable effects to be suppressed during acquisition not occluding details of the data page underneath protective security foil or holograms. On the other hand, when inspecting optically variable devices (OVDs), it is the glare effects which comprise the optical variable response characteristic for the inspected security feature. Hence, the systematic processing of these effects (which is currently not fully supported by devices) can be particularly useful for additional security checks. The difficulty for automated inspection is that an OVD's appearance depends on the document (type and material), specific illumination (type, position and parameters of light sources) and handling (angle between document and light source). Glare effects in document readers can be divided in two categories: (i) internal and (ii) external glare. Internal glare originates from internal non-black parts and the transparent glass window, whereas external glare can refer to OVDs (e.g., holograms) or the document coating and therefore be of interest. Flat field correction (FFC) can help reducing the effect of internal glare. There are two rather different illumination concepts in state-of-the-art document readers targeting the problem to produce a glare-free passport image: dark-field vs. bright field illumination, see also Figure 2.

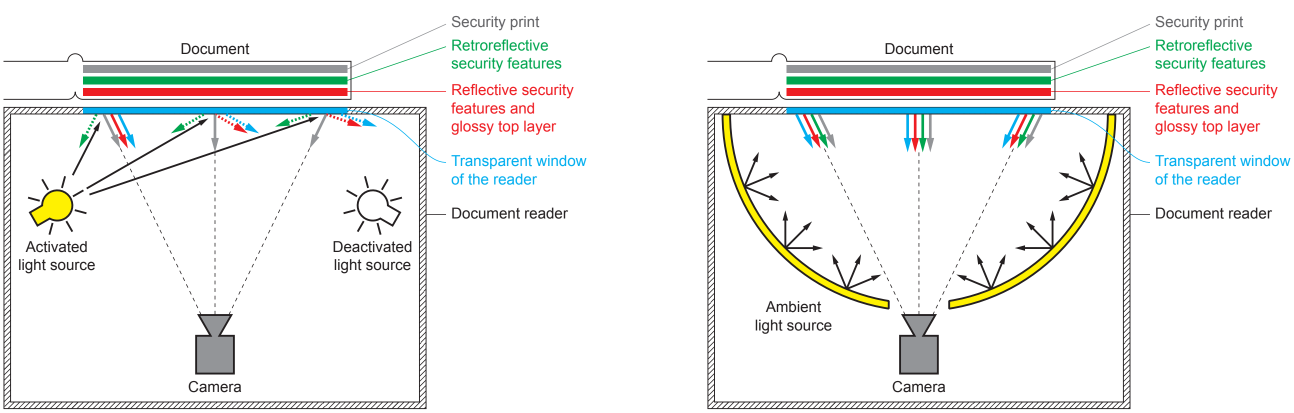

(a) Dark-field Illumination (b) Bright-field Illumination

Figure 2: Dark-field vs. bright-field illumination setup.

(a) Dark-field image without anti-glare

(b) Dark-field image with suboptimal anti-glare

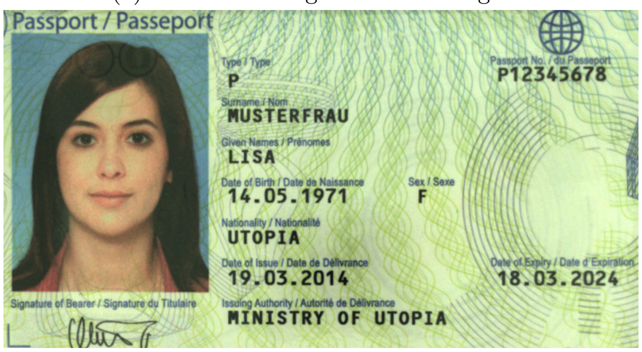

(c) Bright-field image

(d) Dark-field image with good anti-glare

Figure 3: Dark field vs. bright field image examples for a specimen passport crop (no MRZ).

2.1 Dark-field Illumination

In this configuration several small-area light sources such as spots or bar lights are installed inside the document reader (see Figure 2a). As all illuminations employed in this setup take aspecular positions for most imaged locations, reflections are produced in rather limited areas, changing for each light source. At the expense of semi-complex image processing (risk of higher noise, reduced dynamic range), this setup allows for a very efficient suppression of internal as well as external glare, which can be further separated from the ambient response of the document. By combining multiple acquisitions using different light sources, the effect of glare can be significantly reduced, see Figure 3. The difference (reflection image) opens up potential for inspecting OVD security features. However, results naturally depend on the number, location and angles of light sources, relative position of the document and type of holograms (OVD). Note, that the number of illumination sources in state-of-the-art dark-field readers is rather limited (2-4), therefore also limiting the possibilities in glare reduction and inspection of OVDs: If a certain OVD exhibits reflectivity for each of the employed light source positions, its glare can not be removed. On the other hand, if a certain OVD exhibits reflectivity at angles not covered by the available light sources (or due to rotation of the document), it is not visible and cannot be detected.

2.2 Bright-field Illumination

In contrast to the dark-field setup, in bright-field configuration there is just a single large illumination source (indicated by a yellow hemisphere in Figure 2b). This kind of illumination generates a homogenous light similar to daylight, that provides for many illumination directions for the entire scan area. This helps in reducing image processing efforts, preserves high dynamic range and at the same time produces an almost glare-free image in a single acquisition (faster). On the other hand, the ambient response of the document is ultimately mixed with any specular reflections, which may originate from OVDs or other internal/external glare sources. For this reason it is essentially impossible to inspect any OVDs. Colour calibration is possible, but has certain weaknesses due to the mentioned physical constraints. In Figure 3 one can see that glare is almost not visible in the bright-field image, apart from some hologram texture in the upper part of the portrait. There is however and a dark

Table 2: Comparison of different illumination approaches.

Dark-field illumination *Advantages*	**Bright-field illumination** *Advantages*
• efficient anti-glare feature • can detect presence of OVDs • accurate colour calibration	• reduced image processing (preserved dynamic range) • almost glare-free image • single acquisition
Disadvantages	*Disadvantages*
• multiple acquisitions required • using different light sources • more complex image processing (noise)	• more expensive illumination solution • colour calibration with weaknesses • OVD inspection impossible

spot just below the centre of the passport, which is likely due to internal reflections (probably reflection of the camera). This dark spot is not visible in acquisitions of matte surfaces, which shows that this effect is actually dependent on the reflectivity of the inspected surface. Table 2 provides a high-level evaluation of dark-field versus bright-field illumination.

3. DOCUMENT READER CHALLENGE

At AIT we conducted a document reader challenge comparing 9 inspection systems as listed in Table 1 (Fig. 1). Results are anonymised using a permutation of readers referred at as A to I and blind (caption-less) results for device characteristics where there is a risk of deanonymisation. The study aims to provide a holistic view of challenges in the field rather than individual devices. The following sections present the experimental setup and individual device property under test. During the tests only a single parameter is altered at a time keeping all others fixed. Some of the tests or calibrations had to be done in a restricted manner, e.g., image noise measurements or radiometric calibration.

3.1 Setup

Only a single reader offered access to raw sensor data, allowing changed camera settings (e.g., gain and exposure time) and selecting the active image processing operations. Thus, we decided to use the default settings of this reader considering the rest as black-box imaging systems. Table 3 lists hardware and software configuration. For all of the readers the illumination settings were fixed and were directly linked to a predefined set of acquisition types (e.g., VIS, UV, IR, co-axial). Acquisition with switched-off illumination is not specified in guidelines and was not possible for any of the employed devices.

3.2 Optical Resolution

Considering image resolution being crucial for the inspection of small features, such as microprinted text, we used the 1951 USAF 3-bar resolution chart (MIL-STD-150A) for comparing the measurement with the declared value provided by the vendor (see Fig. 4 for crop-out results for individual readers), and to generate modulation transfer function charts. Note, that according to Frontex requirements at least 385 DPI are suggested for document readers employed at border control. The interesting question related to this requirement is that via upscaling methods any target resolution can be matched, however, sensor resolution does not necessarily reflect

Table 3: Hardware and software configuration of tested readers.

	3M AT9000 MK2	**ARH** Combo Smart	**ARH** PRMc	**Bundes-druckerei** VE 600	**DESKO** ICON Gen I	**DESKO** PENTA Gen 4.0	**Regula** 7024m.111	**Regula** 7034.111	**Suprema** RealPass-V
Hardware Serial No.	60A13719	1121299	1151552	349766030	2015 1800163	2015 1800162	7DF299 BA6001	7D9BA0311	956501864
Software Version	3M SDK 3.3.2.7	ARH SDK 2.1.5-25	ARH SDK 2.1.5-25	Visocore 1.8.1	ePassApi 1.0.9	ePassApi 1.0.9	RegulaSDK 4.9.1	RegulaSDK 4.9.1	RealPassSDK 1.9.7

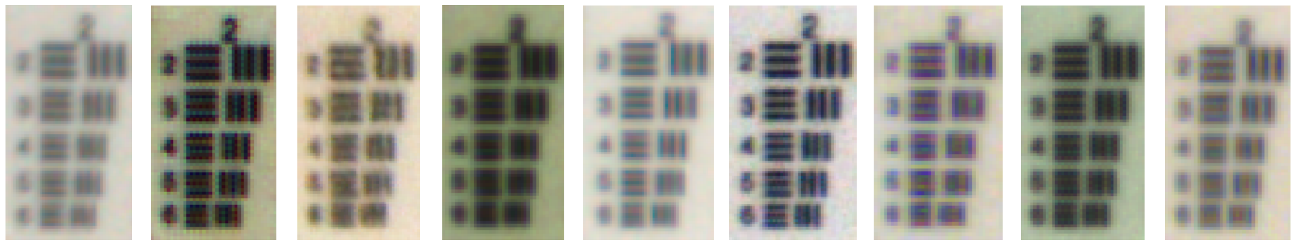

A B C D E F G H I

Figure 4: Crop-outs from the USAF test chart acquired by different readers (A-I).

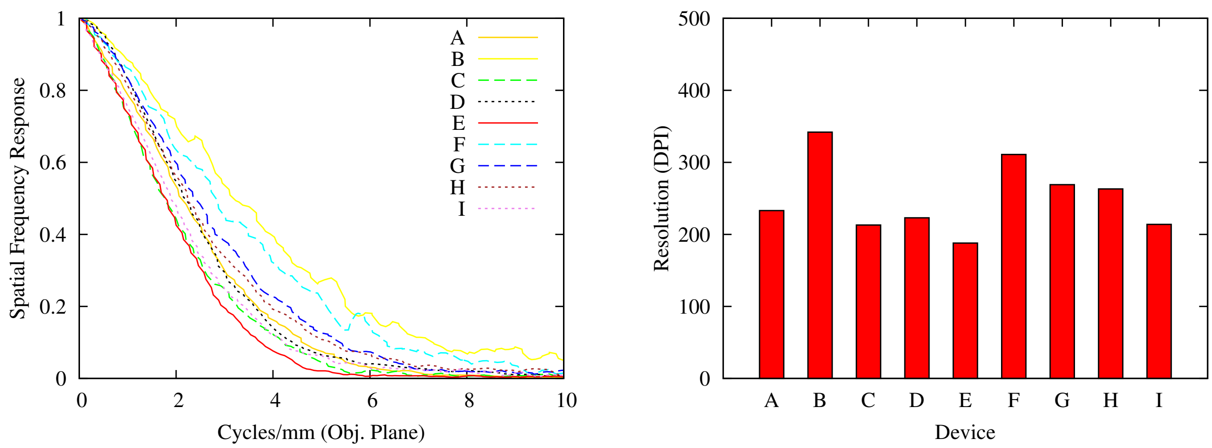

(a) Spatial Frequency Response

(b) Optical resolution from SFR

Figure 5: Optical resolution for different readers (A-I).

true optical resolution. Optical resolution is known to be a much better indicator of performance than a target number of pixels in output images.

There are two basic definitions of image resolution: (i) the size of an area in the object plane that is associated with individual sensor pixels; and (ii) the level of physical detail that is well preserved by the imaging system. The first type of the resolution was assessed by measuring sizes in pixels of objects with precisely known physical dimensions. We found out that the measured sensor resolutions match very well (approx. ±1.2%) with the specification provided by vendors. The second type of resolution was measured by computing the Spatial Frequency Response (SFR) curves using the standard slanted edge approach[12] (see also ISO/IEC 12233). One can see that the tested readers exhibit very diverse resolving power. For example, while in Device F the element 2-6 (i.e., 362.20 DPI) is still readable, in Device C the last readable element is 2-2 (i.e., 228.09 DPI). Quantitative results of the resolution test are shown in Figure 5a. With regards to camera-specific features all measured optical resolutions ranged below 350 DPI, which is, in the extreme case, less than twice below the sensor pixel resolution. There are only two readers (Devices B and F) that satisfy the minimum of 300 DPI recommended in ICAO 9303.[3] According to our experiment no reader was found to be suitable for the inspection of microprinted text security features due to greatly insufficient optical as well as sensor resolution. This highlights potential room for an improvement of employed optical/lens systems used by vendors in general.

3.3 Noise

Low image noise is a prerequisite of successful document verification. In presence of high noise, important image details and fine structures cannot be recovered reliably, which may have negative impact on the verification performance. Microprinted text is an example of a security feature which can be greatly affected by the presence of noise. We measured the image noise assuming its independence from absolute brightness. Noise was assessed in the visible spectrum only in two brightness points (dark and bright) making use of a printed black-and-white checkerboard pattern with and without anti-glare feature turned on. Obtained results are illustrated in Figure

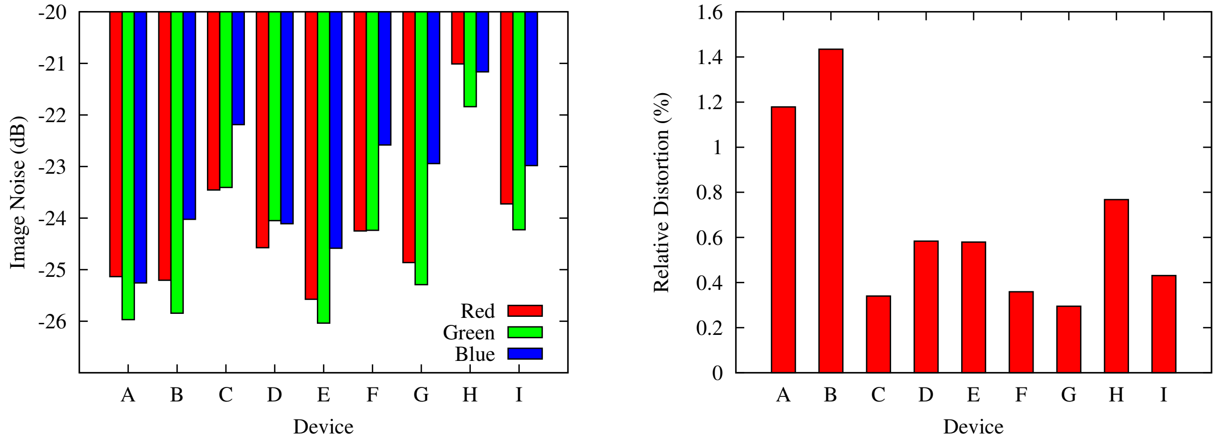

(a) Noise (w/o glare suppression)   (b) Maximum radial distortion

Figure 6: Camera noise and lens geometric distortion results for different readers (A-I).

6a, revealing three groups of readers with slightly different noise levels. The first group composed of the readers A, B, E exhibit low noise around -26dB. The second group including Devices C, D, F, G, I showed medium noise around -24dB, and the Device H showed high noise around -22dB. Moreover, the anti-glare feature tends to increase the image noise levels. This is particularly visible in Device G and I.

3.4 Geometric Distortion

Lens distortion is a monochromatic optical aberration when the lens magnification varies across the field of view at a fixed working distance. The major consequence is that straight lines in the scene are not preserved in the image and appear curved. For simple lenses, two basic types of distortion may arise: barrel and pincushion. In barrel distortion the lines near the edges are curved outwards. In pincushion the lines near the edges are curved inwards. For less corrected lenses, a more complex distortion, for example a wave, may appear.

Lens distortion is usually measured in one of two ways: RIAA TV distortion and radial geometric distortion. For camera-lens combination, when the imaging sensor is not properly aligned with the lens, an additional distortion, called keystone distortion, may appear. The measurement of radial geometric distortion requires a test chart containing a regular grid of geometric objects, for example a checkerboard pattern. The distortion is computed in the following way:

$$D_i = \frac{|H_i' - H_i|}{H_i} \cdot 100, \tag{1}$$

where H_i' is the pixel distance from the image centre to the i-th measured position of a geometric object and H_i is the pixel distance from the image centre to the i-th ideal position in case of undistorted lens. To get a single quantity, the following calculation can be used:

$$D = \underset{i}{max}(D_i), \tag{2}$$

where $\underset{i}{max}(\cdot)$ is the maximum operator (selecting the maximal distortion value over all geometric objects).

Measurements of the lens distortions for the readers under test are shown in Figure 6b. All devices exhibit very low distortion below 1.5% (i.e., invisible for humans). This finding suggests that the readers already include some sort of image undistortion. There are three readers (Devices C, F and G) that exhibit exceptionally low lens distortion below 0.4%.

Geometric distortion correction accounts for compensating local image deformations due to a distorted geometry of the employed optics or the acquisition setup in general. It is particularly important for optical character recognition as well as for other inspection tasks based on pattern matching. Geometric distortions can be suppressed by employing transformations (maps) taking the local and global deviations from the correct geometry into account (i.e., computing intrinsic and extrinsic parameters of the system). This type of correction may have a negative impact on optical resolution, therefore should be considered with care. All tested readers showed very low lens distortions suggesting that further correction is not necessary. However, vendors might already employ geometric calibration (black box setup) as part of their image preprocessing routines.

3.5 Demosaicing

Demosaicing is a standard process in digital imaging to reconstruct a full colour image. The target acquisition of the resolution chart is selected as an indicator to help assessing this behaviour and crop-outs are used for visualization in Figure 4. Regarding the colour reconstruction on digital image sensors, a Colour Filter Array (CFA) is typically used. Using this technique each individual sensor pixel receives its own colour filter (either red, green, or blue), which makes the pixel sensitive to one spectral band only. In most colour image sensors nowadays the so-called Bayer filter mosaic is employed, where a 2×2 pattern of R-, G-, and B-sensitive pixels is repeated throughout the sensor area. In general the Bayer pattern refers to any of the following three cases: RGBG, GRGB, or RGGB, which are typical for having two green pixels. In some cases, where for instance NIR sensitivity is required, one green pixel is replaced by the NIR-sensitive one.

Regardless of the CFA employed, there is always just one spectral channel available for each acquired pixel. In order to reconstruct the colour, all the missing spectral values in each pixel must be derived (reconstructed) from the neighbouring pixels, where the information is available. This technique is called demosaicing and there exist many alternative methods, providing different qualitative results.

There are certain typical artefacts associated with demosaicing, namely zippering, colour moiré, or maze artefacts. We detected strong zippering and colour moiré artefacts in Device B and G, respectively. Moderate demosaicing artefacts were detected in Devices A, E, H, and I. Almost no artefacts were detected in Devices C, D, and F (see also previous Figure 4). Note, that repeated correction might further degrade results therefore suggesting for standardized processing steps for enhanced interoperability.

Eventually, a key observation of this study is the largely neglected employment of colour calibration across devices. A suggestion is to employ colour calibration after FFC using a colour calibration target (e.g., IT8), and measure ΔE values[13] quantifying the perceptual difference / distance between recorded colours.

3.6 Anti-Glare

We investigate both, internal glare effects and glare resulting from OVDs, inspecting how devices deal with this type of disturbance and evaluating whether they have good enough FFC to compensate for glare effects. Figure 7 illustrates differences between isolated glare effects perceived by different readers. It can be seen that there is currently just a minor accordance between glare responses of the same document. OVDs serve as an important

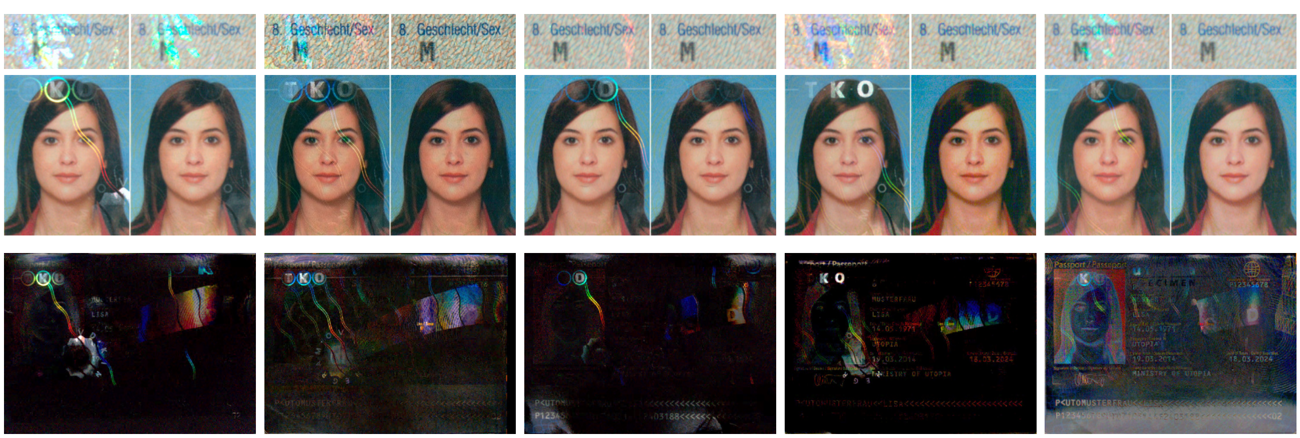

Figure 7: Original (left) and anti-glare enhanced (right) patches with full-page difference (bottom) per reader.

optical security feature. However, they often overlay other parts of the document that are also required for the document's verification (e.g., personalized data or face image). Therefore a well-designed document reader should be able to produce a glare-free (i.e., OVD-free) image for an inspection, ideally with separate reflection image(s) containing the OVD response. In order to allow for an advanced quantitative inspection of OVD security features, it would be necessary to harmonize readers with regards to positions of employed illumination sources and/or employ more accurate image processing methods. Also further standardisation of OVDs at document level would be helpful.

Most of the tested document readers (6 out of 9) featured anti-glare functionality. Glare can be suppressed by either combining multiple images using different illuminations or by employing a bright-field configuration to directly produce a glare-free image. From Figure 7, it can also be seen that the anti-glare efficiency is quite diverse between different devices. We found that 3 out of 6 devices with anti-glare functionality seem to provide consistent glare-free / OVD-free images, all other devices tended to fail in some cases. These findings further support the necessity of harmonization of employed glare processing pipelines in order to guarantee better cross-compatibility between different readers and vendors.

3.7 IR Quality

When visually assessing quality of the infrared acquisitions, we found that most readers compensate quite well for field inhomogeneity (i.e., they seem to apply some sort of FFC already) and directly provide rather even sensitivity across the entire scan area. There are only two readers (Devices D and H) where shading artefacts are clearly visible. The readers mostly differ in the image brightness and contrast as well as in the level of image detail they provide. Some devices seem to be underexposed (Devices B, G, and H), while one device (Device C) generated slightly overexposed IR acquisitions. As for the perceived level of detail, Device B seems to provide the richest data.

In order to explain the observed differences in IR images, we performed a spectroscopic measurement of a dominant wavelength generated by the employed NIR LEDs. The blind results (sorted by value to avoid deanonymization) are summarized in Figure 8a. One can see that most readers (6 out of 9) use NIR LEDs with the wavelength around 850nm. There is one reader employing 880nm LEDs, and two readers employing 930nm LEDs. As we could not detect any apparent correlation between the image quality and dominant wavelength of IR LEDs, we conclude that the observed differences originate from different camera settings as well as calibration and image processing steps taken. Yet another factor, with a potential impact on the IR image quality is likely the position of IR illumination(s), which is not consistent across different vendors and readers.

3.8 UV Quality

In order to investigate the dynamic range of the tested readers in the UV channel, we conducted an experiment with UV-luminescent and UV-dull white papers acquired at the same time. Figure 9 shows examples how

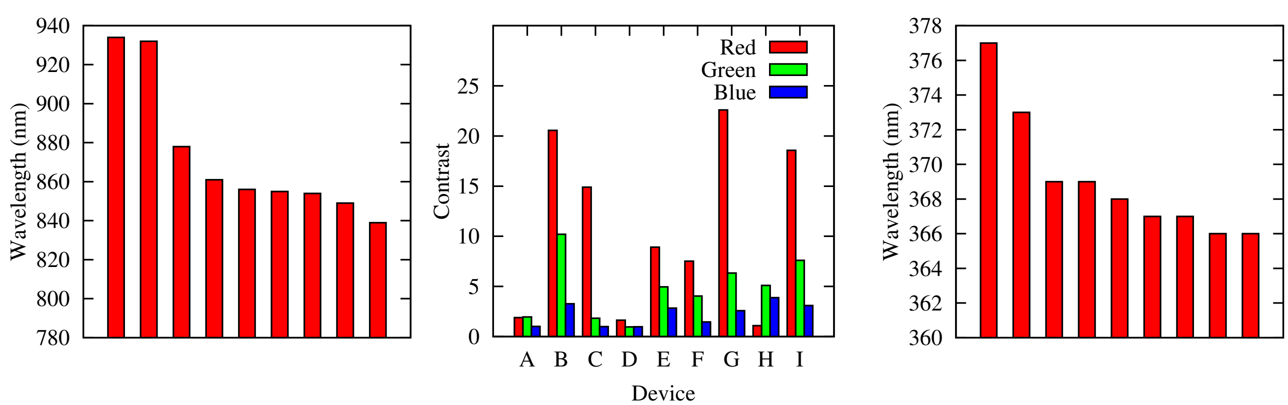

(a) Dominant IR Wavelength (b) UV dull/luminescent Contrast (c) Dominant UV Wavelength

Figure 8: Illumination results for the employed readers (plots (a) and (c) are anonymized).

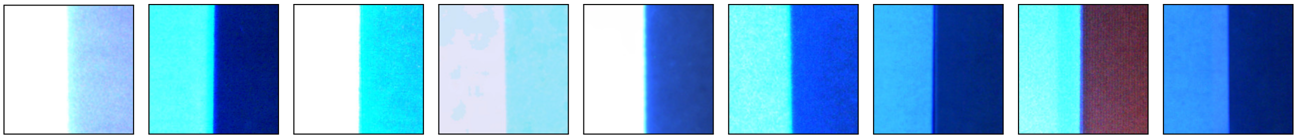

A B C D E F G H I

Figure 9: Appearance of UV-luminescent (left) and UV-dull (right) papers by different document readers.

different the appearance of the same content (UV-luminescent next to UV-dull paper) can be when acquired with various document readers. Also for travel documents it is apparent that UV features differ in almost all aspects, ranging from intensity to colour response. It is quite alarming that the very same security features can be clearly visible in one reader and almost invisible in another. Overall, the worst UV readings were delivered by Device H. Beside the saturation due to overexposure of the UV-luminescent paper (mostly visible in Devices A, C, and E), most readers produced a significant glowing edge around the split between both papers. Quantitative results of this analysis are shown in Figure 8b.

As for the quantitative analysis of the spectral properties of the UV, we measured the dominant wavelength. The obtained blind results (sorted by value to avoid deanonymization) are shown in Figure 8c. Most (7 out of 9) readers employed UV LEDs with the dominant wavelength ranging between 366nm and 369nm. One device employed a 373nm UV LED, while yet another employed a 377nm UV LED. Nevertheless, all these LEDs seem to fall nicely within the UV-A frequency band prescribed by ICAO 9303.[3] Regarding the UV peak width (measured at 50% peak value), different devices seemed to employ different UV band-pass filters in order to shape the UV light emission. The measured bandwidth ranges from 4nm up to over 11nm.

Similar to the analysis of IR illumination, we could not detect any significant correlation between the image quality and spectral properties of UV LEDs. Therefore we believe that the observed differences most likely originate from different camera settings, employed calibration and image processing methods, as well as positioning of the UV illumination.

4. CONCLUSION

In this paper we provided an overview of different device features relevant to output image quality highlighting performance differences between different vendors and device types. While experimental sections provided a detailed view of specific characteristics, main findings and highlights divided into camera-specific and illumination-specific device features, relevant to image quality and interoperability issues, can be summarized as follows: (1) Resolution: With regards to camera-specific features all measured optical resolutions ranged below 350 DPI, which was, in the extreme case, less than twice below the sensor pixel resolution. This highlights a potential room for an improvement of employed optical/lens systems used by vendors in general. No reader was suitable for the inspection of microprinted text security features due to greatly insufficient optical as well as sensor resolution. (2) Calibration: Despite the image noise tended to increase with the glare reduction turned on, using

Table 4: Non-exhaustive list of subjective quantification of test results obtained for individual tested readers.

	Res.	**Noise**	**Demosaicing**	**Anti-glare**	**Shading Calib.**	**IR-Quality**	**UV-Quality**
A	low	low	medium moiré	insufficient	difficult with glare	good	low contrast
B	high	low	strong zippering	good	possible	slightly underexposed	good
C	low	med	good	poor	difficult with glare	slightly overexposed	good
D	low	med	good	good	difficult with glare	minor shading artefacts	low contrast
E	low	low	medium moiré	insufficient	difficult with glare	good	good
F	high	med	good	poor	difficult with glare	good	good
G	med	med	strong moiré	good	possible	slightly underexposed	good
H	med	high	zippering	poor	difficult with glare	underexp., shading artefacts	poor, low contrast
I	low	med	medium moiré	good	possible	good	good

this feature is highly recommended due to its essential role in enabling the colour calibration and consequently any colour-based inspection. We detected very low geometric distortion for all readers under test. (3) Visible illumination: The dark-field setup has some potential for future automated inspection of OVDs, whereas bright-field images tended to produce visually appealing results excellent for manual inspection at the expense of more difficult colour calibration. Furthermore we also found the axial illumination useful for further security and material checks. (4) IR / UV illumination: For most tested readers, the optical characteristics of UV and IR illumination sources were in a narrow band, which did not explain observed strong quality differences in obtained images. Besides different camera settings, calibration and image processing steps, an important hardware difference between the tested readers was the position of UV and IR illuminations. We believe that this might be one of the main factors influencing the output image quality in both spectral channels. (5) Interoperability: Appropriate calibration steps are crucial for interoperability of different document readers. In particular, the anti-glare feature proved to be inevitable for proper colour calibration when dealing with documents with glossy parts.

Table 4 provides a non-exhaustive list of test results obtained for individual tested readers. In the future, we will focus on quality metrics and methods to normalize input images for increased interoperability.

ACKNOWLEDGMENTS

This project has received funding from the European Union's Seventh Framework Programme for research, technological development and demonstration under grant agreement no 312583.

REFERENCES

[1] Gariup, M. and Soederlind, G., "Document fraud detection at the border: Preliminary observations on human and machine performance," in [*Proc. Europ. Intelligence and Security Informatics Conference (EISIC)*], 231–238 (Aug 2013).

[2] Frontex, "The document challenge II: Testing human and machine performance in detecting and classifying genuine and false travel documents," report 2015-08-18, Frontex Research and Development Unit (2015).

[3] ICAO, "Machine readable travel documents - machine readable passports," Doc-9303, 7th Ed., International Civil Aviation Organisation (2015).

[4] Ness, W., "Method and device for checking an electronic passport," Patent US 8857717, Giesecke and Devrient (2006).

[5] Butt, M., Marti, S., Nouak, A., Koplin, J., Raghavendra, R., and Li, G., "Towards e-passport duplicate enrollment check in the european union," in [*Proc. Europ. Intelligence and Security Informatics Conference (EISIC)*], 247–251 (Aug 2013).

[6] Hamad, F., Zraqou, J., Maaita, A., and Taleb, A. A., "A secure authentication system for epassport detection and verification," in [*Proc. Europ. Intelligence and Security Informatics Conference (EISIC)*], 173–176 (Sept 2015).

[7] Monnerat, J., Vaudenay, S., and Vuagnoux., M., "About machine-readable travel documents: Privacy enhancement using (weakly) non-transferable data authentication.," in [*Proc. RFID Security Workshop (RFIDSec)*], 15–28 (2007).

[8] Kundra, S., Dureja, A., and Bhatnagar, R., "The study of recent technologies used in e-passport system," in [*Proc. IEEE Global Hum. Techn. Conf. - South Asia Satellite (GHTC-SAS)*], 141–146 (Sept 2014).

[9] Dolev, G., "Apparatus and methods for computerized authentication of electronic documents," Patent WO 2011058553, Au10Tix (2010).

[10] Blair, R. B., "Systems and methods for spectral authentication of a feature of a document," Patent WO 2014021976, De La Rue (2013).

[11] Sinha, A., "A survey of system security in contactless electronic passports," *J. Comput. Secur.* **19**, 203–226 (Jan. 2011).

[12] Burns, P., "Slanted-edge mtf for digital camera and scanner analysis," in [*Proc. Image Proc., Image Quality, Image Capture, Systems Conf. (PICS)*], 135–138 (Mar 2000).

[13] Valberg, A., [*Light Vision Color*], Wiley (2005). ISBN 0470849029.